2019 IEEE/RSJ International Conference on Intelligent Robots and Systems (IROS)
Macau, China, November 4-8, 2019

Adaptive swept volumes generation for human-robot coexistence using Gaussian Processes

Andrea Casalino[1], Alberto Brameri[1], Andrea Maria Zanchettin[1] and Paolo Rocco[1]

***Abstract*— Letting humans and robots share a common space for collaboration is considered a consolidated practice. The trajectories followed by the robot must be safe for the human mate, especially when the robot holds dangerous tools or parts. At the same time, the productivity must be preserved, without imposing too restrictive limitations on the robot's movements. This article proposes the use of Gaussian Processes to predict the motion of an operator in a robotic cell, with the aim of controlling the robot speed and avoid collisions. An adaptive approach is proposed and the model for the human motion is persistently re-updated. The resulting approach will be demonstrated to be less conservative than previous ones, while at the same time to preserve the safety of the operator. Real experiments have been conducted on the 7 d.o.f. ABB YuMi robot.**

I. Introduction

The industrial collaborative robots market has been growing over the years. These robots also called cobots, are specifically designed to work with humans, since they are lighter, without edges, sometimes covered with paddings to damp the effects of impacts, and often equipped with kinematic redundancy (i.e. they have a number of joints greater than the strictly necessary one) [1]. They are conceived to work closely to humans in modern production plants, providing assistance. This is far from the old paradigm adopted for industrial robots, which were placed in protected environments by means of physical infrastructures (fences or optical barriers). Moreover, a significant effort was spent during past years to develop control strategies allowing also standard non-collaborative robots to work close to humans without the need of being segregated ([2] and [3]).

Both for collaborative and standard robots, one fundamental step to achieve the coexistence with humans in a shared space is to perceive them. Information coming from sensors are then considered by motion controllers. High-visibility industrial clothing detection strategies based on RGB and IR cameras have been proposed in [4], while [5] introduced the concept of "smart floor" by adopting pressure-sensitive sensors to keep track of human motions. RGB-D cameras have been exploited in [6]. Regarding motion control, [10] introduced a safety constraint regulating the robot speed along an assigned path. The approach was then extended in [11], introducing "Swept Volumes": portions of the environment, containing the human predicted motion, which are treated like obstacles to avoid. Predicting in a reliable way the human motion is therefore critical to apply the aforementioned method. To this purpose, Gaussian Processes (GPs) have been already proved to be effective. In [7], the 3D people tracking problem is addressed: GPs provide prior knowledge to compensate for occlusions and noise. The method proposed in [8] exploits a GP in conjunction with an Unscented Kalman Filter for motion tracking, while [9] adopts GPs for activity classification. However, it is difficult to find strategies that refine a predictive model on-line, since usually learning relies on huge training sets, typically processed off-line.

The main contribution of this work is the proposal of an adaptive method to model the human motion when this latter collaborates with a robot, relying on Gaussian Processes. The motion of the robot is controlled as similarly done in [11] but considering a predictive model tailored to specific subject for the computation of swept volumes. This results in a reduced conservativeness that improves the speed of the robot. The rest of this article is structured as follows. Section II will briefly review some prior results regarding motion control for cobots. Section III will review the basic mechanism of Gaussian Processes, while the proposed approach is detailed in Section IV. Section V will present some validating results, while Section VI will give some concluding considerations.

II. Safe motion control of cobots

The technique proposed in [11] for the computation of human swept volumes is briefly reviewed in this Section. The human is treated like a manipulator, whose motion is described by a 12 d.o.f. kinematic model. $\underline{q} = \begin{bmatrix}\underline{q}_{base} & \underline{q}_{armR} & \underline{q}_{armL}\end{bmatrix}$ is the vector describing the human posture. $\underline{q}_{base} = \begin{bmatrix}q_1 & q_2 & q_3 & q_4\end{bmatrix}$ contains the position and orientation of the torso, while $\underline{q}_{armR} = \begin{bmatrix}q_5 & q_6 & q_7 & q_8\end{bmatrix}$ describes the posture of the right arm of the operator, similarly $\underline{q}_{armL} = \begin{bmatrix}q_9 & q_{10} & q_{11} & q_{12}\end{bmatrix}$ for the left arm.

A depth camera is able to provide on-line the position of some skeletal points of interest, which are used together with an inverse kinematic function to compute $\underline{q}$, see [10] for further details. By considering some kinematic limitations for the human motion (maximal and minimal joint velocities and accelerations) it is possible to compute the reachable set of every joint, represented by $\underline{\Delta}^+$ and $\underline{\Delta}^-$. The latter quantities are, respectively, the maximal and minimal possible excursions that human articulations can undergo within a prediction time T starting from the current one. More formally, for the generic j^{th} joint:

$$\begin{cases}\Delta_j^+ = min \quad \Delta \quad s.t. \\ \Delta \geq 0 \quad \bigwedge \quad q_j(t+\delta t) < q_j(t) + \Delta \quad \forall \delta t \in [0, T]\end{cases}$$

[1] The authors are with Politecnico di Milano, Dipartimento di Elettronica, Informazione e Bioingegneria, Piazza L. Da Vinci 32, 20133, Milano, Italy (e-mail: name.surname@polimi.it).

$$\begin{cases} \Delta_j^- = min \quad \Delta \quad s.t. \\ \Delta \geq 0 \quad \bigwedge \quad q_j(t+\delta t) > q_j(t) - \Delta \quad \forall \delta t \in [0, T] \end{cases} \tag{1}$$

$\underline{\underline{\Delta}}^+$ and $\underline{\underline{\Delta}}^-$ are considered to compute the swept volumes, by following the method adopted in [12]. Such shapes are treated like obstacles that need to be avoided, thus ensuring the human safety.

The method proposed in [11] is effective in guaranteeing the safety, but seems to be very conservative when computing $\underline{\underline{\Delta}}^+$ and $\underline{\underline{\Delta}}^-$, since the kinematic limitations considered are not tailored to specific subjects. The aim of this work is instead to exploit Gaussian Processes to forecast the evolution of $\underline{q}$ in order to compute $\underline{\underline{\Delta}}^+$ and $\underline{\underline{\Delta}}^-$ in a less conservative way.

III. Gaussian Processes

Gaussian Processes [13], are typically adopted to learn unknown functions from samples. Suppose to have a function $g : \mathcal{X} \rightarrow \mathcal{F}, \mathcal{X} \subseteq \mathcal{R}^d, \mathcal{F} \subseteq \mathcal{R}$, which is unknown. The only information available about g is represented by a certain number N of samples $\{\langle \underline{X}_1, f_1 \rangle, \cdots, \langle \underline{X}_N, f_N \rangle\}$, where $f_j = g(\underline{X}_j) + r$, with r represents noise. Since all $f_{1,\cdots,N}$ are generated by the same function g, they are correlated. To describe such a correlation, GPs assume a certain prior knowledge about g, by considering a kernel function $\boldsymbol{K}(\underline{\underline{X}}, \underline{\underline{X}})$, which is a symmetric positive definite matrix, such that:

$$\begin{bmatrix} f_1(\underline{\underline{X}})_{prior} & \cdots & f_N(\underline{\underline{X}})_{prior} \end{bmatrix}^T \backsim \mathcal{N}(0, \boldsymbol{K}(\underline{\underline{X}}, \underline{\underline{X}})) \tag{2}$$

where matrix $\underline{\underline{X}} = \begin{bmatrix} \underline{X}_1^T & \cdots & \underline{X}_N^T \end{bmatrix}^T$, contains every input in the training set. $\underline{F} = \begin{bmatrix} f_1 & \cdots & f_N \end{bmatrix}^T$ is instead used to group all outputs in the same set. Common kernel functions adopted are Radial Basis Function, Rational Quadratic kernel, Linear kernel, Periodic kernel, etc. [13]. For the purpose of this work, we will consider a kernel function $\boldsymbol{K}$ composed as follows:

$$\begin{aligned} \boldsymbol{K} &= \boldsymbol{K}1 + \boldsymbol{K}2 + \boldsymbol{K}3 \\ K1_{i,j} &= \theta_3 exp\left(-\frac{\theta_2}{2}\|\underline{X}_i - \underline{X}_j\|_2^2\right) \\ K2_{i,j} &= \theta_1 \underline{X}_i \underline{X}_j^T \\ K3_{i,j} &= \frac{1}{\theta_4}\delta_{i,j} \end{aligned} \tag{3}$$

with $\delta_{i,j}$ equal to the Kronecker delta. The parameters $\underline{\Theta} = \begin{bmatrix} \theta_1 & \cdots & \theta_4 \end{bmatrix}^T$ involved in the computation of $\boldsymbol{K}$ are called hyperparameters and their values are determined maximising the likelihood of the training set, i.e:

$$\underline{\Theta} = \underset{\underline{\Theta}}{\operatorname{argmax}} \left[\left(\sum_{k=1}^{N} \mathbb{P}(f_k(\underline{\underline{X}}, \underline{\Theta})_{prior}) \right) \mathbb{P}(\underline{\Theta})_{prior} \right] \tag{4}$$

A prediction about the value assumed by g for an input $\underline{\chi}$ not contained in the training set $\underline{\underline{X}}$ can be made by considering the joint probability of $\underline{\underline{X}}$ and $\underline{\chi}$. Indeed, it holds that:

$$\begin{bmatrix} f \\ \underline{F} \end{bmatrix}_{prior} \backsim \mathcal{N}(\begin{bmatrix} 0 \\ 0 \end{bmatrix}, \hat{\boldsymbol{K}})$$
$$\hat{\boldsymbol{K}} = \begin{bmatrix} \boldsymbol{K}(\underline{\chi}, \underline{\chi}) & \boldsymbol{K}(\underline{\chi}, \underline{\underline{X}}) \\ \boldsymbol{K}(\underline{\underline{X}}, \underline{\chi}) & \boldsymbol{K}(\underline{\underline{X}}, \underline{\underline{X}}) \end{bmatrix} \tag{5}$$

Therefore, the prediction is made considering the conditional distribution of probability of f w. r.t. the training set, leading to:

$$\begin{aligned} f &= g(\underline{\chi})_{post} \backsim \mathcal{N}(\underline{\mu}_\chi, \Sigma_\chi) \\ \Sigma_\chi &= (\boldsymbol{K}(\underline{\chi}, \underline{\chi}) - \boldsymbol{K}(\underline{\chi}, \underline{\underline{X}})\boldsymbol{K}(\underline{\underline{X}}, \underline{\underline{X}})^{-1}\boldsymbol{K}(\underline{\chi}, \underline{\underline{X}})^T) \\ \underline{\mu}_\chi &= (\boldsymbol{K}(\underline{\chi}, \underline{\underline{X}})\boldsymbol{K}(\underline{\underline{X}}, \underline{\underline{X}})^{-1}\underline{F})^T \end{aligned} \tag{6}$$

The Gaussian process g_{GP}, whose training set is $\underline{\underline{X}}$,$\underline{F}$ and hyperparameters are $\underline{\Theta}$, is used to approximate g. The following notation will be adopted in the sequel: $g \doteq g_{GP}(\underline{\chi})$, which implies to obtain g by sampling from the distribution $\mathcal{N}(\underline{\mu}_\chi, \Sigma_\chi)$. The aforementioned considerations can be extended to multidimensional functions, but we omit here the details.

IV. Proposed method

The aim of this Section is to show how Gaussian Processes can be exploited to compute customized models of human motion, tailored to specific subjects. We assume every operator present in a cell is monitored by a surveillance camera, able to provide an estimate of the operator's posture $\underline{q}$ at a certain sampling frequency $1/\Delta t$. Let $\underline{\phi}_k$ denote the state of the operator's articulations at step k:

$$\underline{\phi}_k = \begin{bmatrix} \ddot{\underline{q}}_k^T & \dot{\underline{q}}_k^T & \underline{q}_k^T \end{bmatrix}^T \tag{7}$$

$\underline{\phi}_k$ can be estimated applying a Kalman filter on a linear kinematic model made of a chain of three integrators:

$$\begin{aligned} \underline{\phi}_{k+1} &= \underline{\underline{A}}\,\underline{\phi}_k + \underline{w} \\ \underline{z}_{k+1} &= \underline{q}_{k+1} = \begin{bmatrix} 0 & 0 & \underline{\underline{I}} \end{bmatrix} \underline{\phi}_k + \underline{e} \\ \underline{\underline{A}} &= \begin{bmatrix} \underline{\underline{I}} & \underline{\underline{0}} & \underline{\underline{0}} \\ \Delta t \underline{\underline{I}} & \underline{\underline{I}} & \underline{\underline{0}} \\ 0.5\Delta t^2 \underline{\underline{I}} & \Delta t \underline{\underline{I}} & \underline{\underline{I}} \end{bmatrix} \end{aligned} \tag{8}$$

where $\underline{w}$ and $\underline{e}$ are the process and the measurement noise respectively, which are assumed to be Gaussian. The classical forward formulation of the Kalman filter is able to provide recursively $\underline{\boldsymbol{\phi}}_{k|k}$, i.e. the mean of the posterior distribution of the state $\underline{\boldsymbol{\phi}}_k$, conditioned to all the measures seen in the past $\underline{z}_{1,\cdots,k}$. In [11], the estimate $\underline{\phi}_{k|k}$, is taken into account for computing the reachable sets of every q_i, by assuming the accelerations $\ddot{\underline{q}}$ and the velocities $\dot{\underline{q}}$ are bounded. The aforementioned sets are then considered for the swept volumes computation. However, the kinematic limitations adopted are not tailored to specific subjects, but worst case values are used.

However, in collaborative contexts we can assume the human motion to have some kind of periodicity, since the human and the robot have to alternatively accomplish a certain number

of operations to assemble some kind of products for example. In similar scenarios the worst case approach of [11] produces unnecessary conservative predictions.

On the opposite, the aim of this work is to model the aforementioned periodicity, for providing more accurate medium-term predictions. Such predictions cannot be extracted from the purely linear model expressed in equation (8), which can be only adopted for filtering the observations. However, the estimates $\underline{\boldsymbol{\phi}}_{k|k}$ provided by the Kalman filter are exploited to refine a Gaussian Process able to efficiently describe the human motion. An adaptive approach is used, starting from an initial model and continuously refining it at a certain frequency. Let h be the function governing the periodicity of the human motion. The definition of h is:

$$\underline{\phi}_k = h(\underline{\phi}_{k-1}, \cdots, \underline{\phi}_{k-P}) \tag{9}$$

where P is the order of the model. h is clearly unknown, but can be approximated by making use of a Gaussian Process h_{GP}:

$$h(\underline{\phi}_{k-1}, \cdots, \underline{\phi}_{k-P}) \doteq h_{GP}(\underline{\phi}_{k-1}, \cdots, \underline{\phi}_{k-P}) \tag{10}$$

We will propose in the sequel three different possible ways to build h_{GP}. As exposed in Section III, Gaussian Processes rely on samples. In particular, we propose to use as samples for h_{GP}, not the on-line computed estimates $\underline{\phi}_{k|k}$, but $\underline{\phi}_{k|K}$, i.e. the mean of the posterior distribution of $\underline{\phi}_k$ conditioned to all measures in a window: $\underline{z}_{1,\cdots,ki,\cdots,kf}$.

Therefore, the proposed approach periodically updates h_{GP}, reasoning on the most recent available window of recent observations. The frequency of the model update is clearly lower than $1/\Delta t$, i.e. the sampling time adopted for updating the human state, which is also the sampling time adopted for updating the swept volumes $\underline{\Delta}^+$ and $\underline{\Delta}^-$. At every step k, $\underline{\Delta}_k^+$ and $\underline{\Delta}_k^-$ are recomputed on the basis of the most recent learnt h_{GP}.

The computation of $\underline{\phi}_{k|K}$ is made applying the backward formulation of the Kalman filter (see [15] at Section 3.6.1), on the window $ki, \cdots, kf$, leading to:

$$\begin{aligned} \underline{\phi}_{k+1|k} &= \underline{\underline{A}}\underline{\phi}_{k|k}; \quad \underline{\underline{V}}_{k+1|k} = \underline{\underline{A}}\underline{\underline{V}}_{k|k}\underline{\underline{A}}^T + \underline{\underline{W}} \\ \underline{\underline{J}}_k &= \underline{\underline{V}}_{k|k}\underline{\underline{A}}^T\underline{\underline{V}}_{k+1|k}^{-1} \\ \underline{\phi}_{k|K} &= \underline{\phi}_{k|k} + \underline{\underline{J}}_k(\underline{\phi}_{k+1|K} - \underline{\phi}_{k+1|k}) \end{aligned} \tag{11}$$

where $\underline{\underline{W}}$ is the covariance of $\underline{w}$, while $\underline{\underline{V}}_{k|k}$ is the covariance of the posterior distribution of $\underline{\phi}_k$, conditioned to the measures $\underline{z}_{1,\cdots,k}$. Both $\underline{\phi}_{k|k}$ and $\underline{\underline{V}}_{k|k}$ are computed on-line during the canonical application of the Kalman filter, therefore those quantities are already known when updating the model. Expressions in equation (11) are applied recursively backwards in time. The estimates $\underline{\phi}_{ki|K,\cdots,kf|K}$ are manipulated in a proper way, to obtain new samples for enriching the training set of h_{GP}, see Sections IV-A, IV-B and IV-C.

The way h_{GP} is adopted for computing human swept volume is now detailed. The computation of $\underline{\Delta}_k^+$ is made considering a prediction horizon of a certain length M, the computation of $\underline{\Delta}_k^-$ is similar. Since GPs are stochastic models, we have to deal with uncertainties. This is addressed by computing $\underline{\Delta}_k^+$ as a result of a Monte Carlo simulation consisting of T trials. Every trial starts from $\underline{\phi}_{k|k}$ and propagates it M times by using h_{GP}, obtaining a sampled trajectory $\underline{\underline{Q}}_t$. For the t^{th} trial, $\underline{\tilde{\Delta}}_t^+$ is computed considering the maximal excursion reached by every joint. Finally, $\underline{\Delta}^+$ is taken as the mean of every $\underline{\tilde{\Delta}}_t^+$. More formally, for every trial t, it is necessary to sample a trajectory $\underline{\underline{Q}}_t$ and compute $\underline{\tilde{\Delta}}_t^+$ as follows:

$$\begin{aligned} \underline{\underline{Q}}_t &= \begin{bmatrix} \underline{q}_{k|k} & \underline{\tilde{q}}_{k+1} & \underline{\tilde{q}}_{k+2} & \cdots & \underline{\tilde{q}}_{k+M} \end{bmatrix} \\ \underline{\tilde{\phi}}_{k+l} &\doteq h_{GP}(\underline{\tilde{\phi}}_{k+l-1}, \cdots, \underline{\tilde{\phi}}_{k+l-P}) \ \forall l = 1, \cdots, M \\ \tilde{\Delta}_{j\,t}^+ &= \mathbf{max}(0, \mathbf{max}(q_{j\,k}, \tilde{q}_{j\,k+1}, \cdots, \tilde{q}_{j\,k+M}) - q_{j\,k}) \\ \underline{\tilde{\Delta}_t^+} &= \begin{bmatrix} \tilde{\Delta}_{1\,t}^+ & \cdots & \tilde{\Delta}_{12\,t}^+ \end{bmatrix}^T \end{aligned} \tag{12}$$

In the above equation every $\underline{\tilde{\phi}}_{k+p}$ (with p negative or null) is assumed to be equal to $\underline{\phi}_{k+p|k+p}$. The predicted $\underline{\Delta}_k^+$ is computed as the mean of the trials:

$$\underline{\Delta}_k^+ = \frac{1}{T}\sum_{t=1}^{T} \underline{\tilde{\Delta}_t^+} \tag{13}$$

The entire pipeline of the approach is reported in Fig. 1. The following Subsections illustrate three possible ways to model h_{GP}.

A. Model A, decentralized approach

The first possible model makes 12 independent predictions, one for each human articulation. Indeed, for every joint only the previous accelerations, velocities and positions are considered to make a prediction about the future trajectory. This is equivalent to have 12 independent GPs assembled together to form h_{GP}. For notational purposes, let $\underline{\varphi}^j$ denote the state of the j^{th} joint:

$$\underline{\varphi}^j = \begin{bmatrix} \ddot{q}_j & \dot{q}_j & q_j \end{bmatrix}^T \tag{14}$$

The GP modelling the evolution in time of $\underline{\varphi}^j$ is a function:

$$\underline{\varphi}_k^j \doteq h_{GP}^j(\underline{\varphi}_{k-1}^j, \cdots, \underline{\varphi}_{k-P}^j) \tag{15}$$

The comprehensive prediction about $\underline{\phi}$ is obtained by assembling in the proper way every predicted $\underline{\varphi}^j$. Every h_{GP}^j is updated separately, adding to the training set, a set of new samples $\{\cdots, \langle \underline{X}_l, \underline{F}_l \rangle, \cdots\}$, with the generic $\underline{X}_l$ and $\underline{F}_l$ equal to:

$$\underline{F}_l = \underline{\varphi}_{k|K}^{j\,T} \qquad \underline{X}_l = \begin{bmatrix} \underline{\varphi}_{k-1|K}^{j\,T} & \cdots & \underline{\varphi}_{k-P|K}^{j\,T} \end{bmatrix} \tag{16}$$

B. Model B, centralized approach

The decentralized model introduced before is able to express the periodicity of human motion. However, such motion usually evolves in a coordinated way among the articulations. For this reason, it seems more natural to consider a model constituted by a single GP, that takes into account the past

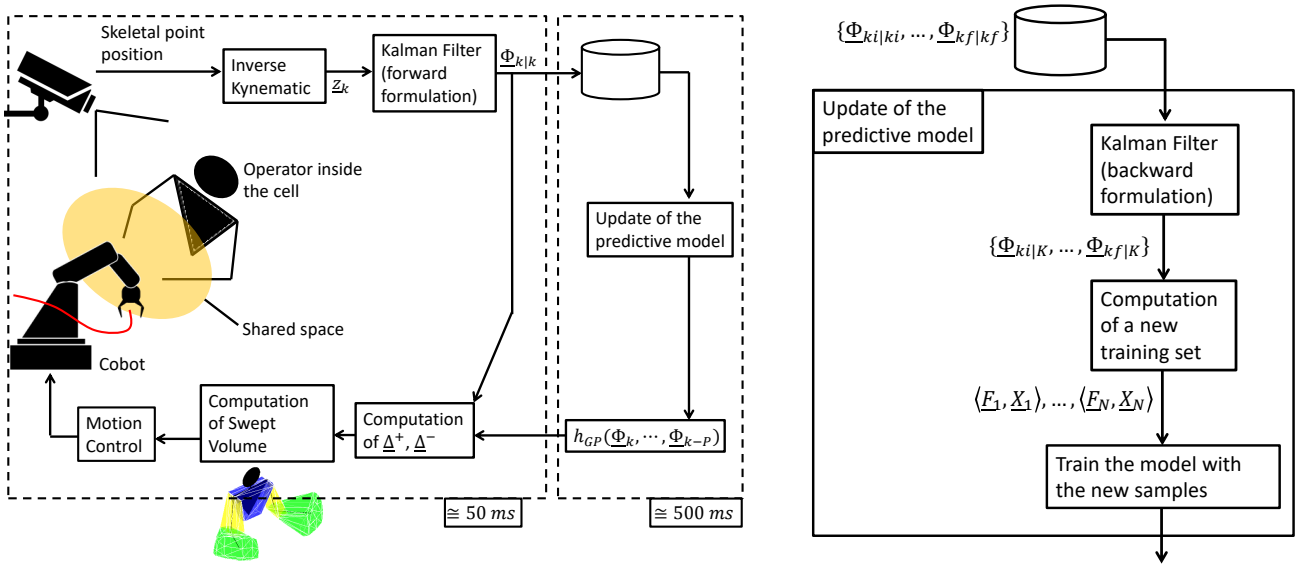

Fig. 1: Pipeline describing the developed approach. The picture on the right details the steps involved for updating h_{GP}, i.e. the model describing human motion.

evolution of the entire state $\underline{\phi}$ when making a prediction for every joint.

$$\underline{\phi_k} \doteq h_{GP}(\underline{\phi}_{k-1}, \cdots, \underline{\phi}_{k-P}) \tag{17}$$

Notice that in this case the computational effort required to update the model and compute $\underline{\Delta}^+$, $\underline{\Delta}^-$ is significantly higher than a purely decentralized approach, since the complexity of GP scales quadratically with the cardinality of the domain of the function to approximate.

C. Model C, hybrid approach

The centralized model introduced before is meant to represent the coordination existing between the articulations. However, it is also computationally heavy. Moreover, the actual coordination governing human motion involves groups of joints. For example, when the operator moves his/her arms, joints of the left arm are moved independently from the ones of the right. For this reason, we can think of a third kind of model that represents separately three main groups of articulations: the moving base, the right arm and the left one. $\underline{\alpha}, \underline{\beta}$ and $\underline{\gamma}$ denotes the state of the three groups of joints:

$$\underline{\alpha} = \begin{bmatrix} \underline{\ddot{q}}_{base\,k} \\ \underline{\dot{q}}_{base\,k} \\ \underline{q}_{base\,k} \end{bmatrix}; \quad \underline{\beta} = \begin{bmatrix} \underline{\ddot{q}}_{armR\,k} \\ \underline{\dot{q}}_{armR\,k} \\ \underline{q}_{armR\,k} \end{bmatrix}; \quad \underline{\gamma} = \begin{bmatrix} \underline{\ddot{q}}_{armL\,k} \\ \underline{\dot{q}}_{armL\,k} \\ \underline{q}_{armL\,k} \end{bmatrix} \tag{18}$$

The prediction about $\underline{\phi}$ is the assembly of three independent predictions:

$$\underline{\alpha_k} \doteq h^{\alpha}_{GP}(\underline{\alpha}_{k-1}, \cdots, \underline{\alpha}_{k-P}) \tag{19}$$

$$\underline{\beta_k} \doteq h^{\beta}_{GP}(\underline{\beta}_{k-1}, \cdots, \underline{\beta}_{k-P}) \tag{20}$$

$$\underline{\gamma_k} \doteq h^{\gamma}_{GP}(\underline{\gamma}_{k-1}, \cdots, \underline{\gamma}_{k-P}) \tag{21}$$

h^{α}_{GP}, h^{β}_{GP} and h^{γ}_{GP} are updated considering three independent newer training sets.

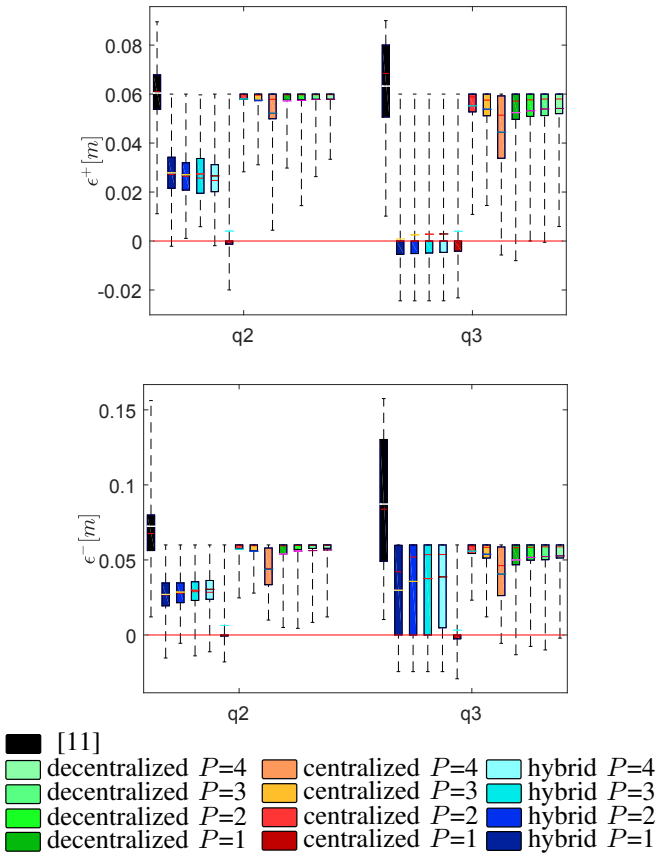

Fig. 2: Distributions of ϵ^+ and ϵ^-, for joint q_2 and q_3 of the kinematic model presented in Section II. The red horizontal line, divide conservative predictions from the ones for which a violation happens. Results for similar joints of both arms are condensed in a single boxplot.

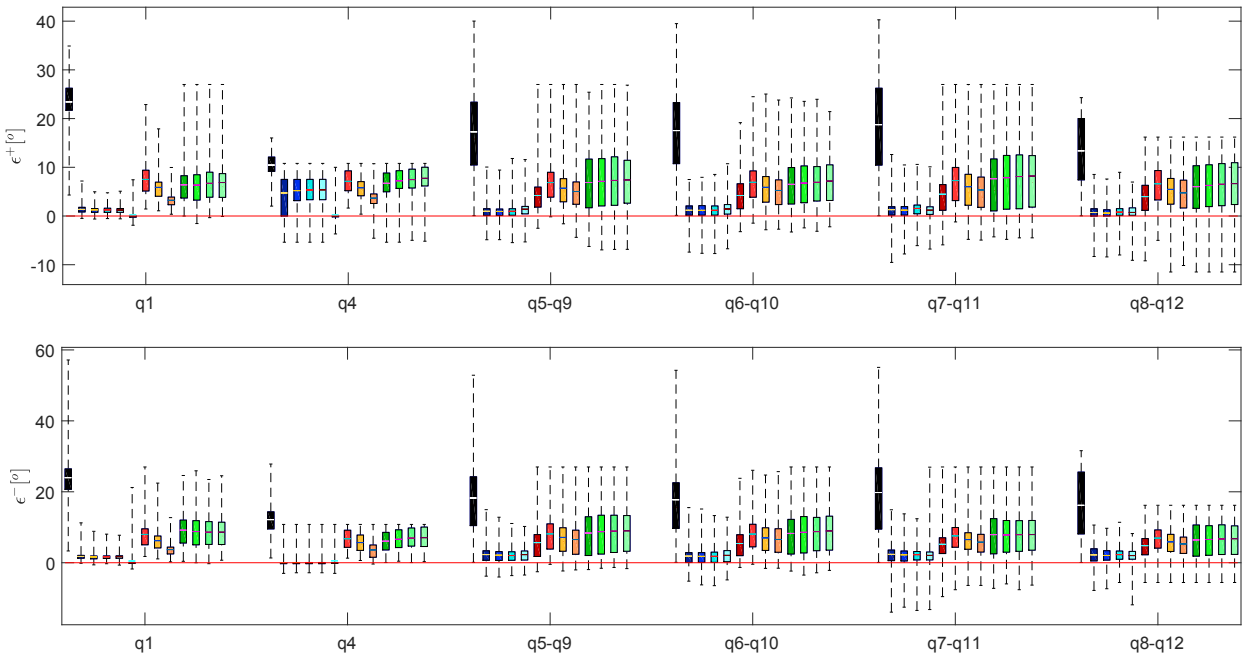

Fig. 3: Distributions of ϵ^+ and ϵ^-, for joints $q_{1,4,5,6,7,8,9,10,11,12}$ (i.e. the rotating ones) of the kinematic model presented in Section II. Results for similar joints are condensed in a single boxplot. The same legend in Figure 2 applies.

V. Experiments

The experimental set-up adopted is reported in Figure 4a. The Kinect reported in the same Figure is exploited to perceive the posture of the human during the time. This information is sent to a CPU, which is also connected to YuMi. The robot speed is modulated as done in [10]. At every steps, the convex shapes representing the swept volumes are recomputed by the CPU connected to robot. Such volumes are exploited for defining a constrained optimization problem whose solution is used for modulating the the robot speed along its current assigned path. The aim is to compute the maximal speed to set for avoiding collisions with the aforementioned swept volumes (in case of critical circumstances, the robot motion can be also interrupted). Clearly, a less conservative computation of human swept volumes leads to reduced size obstacles to avoid, allowing a greater cruise speed.

A human operator and YuMi are required to simultaneously assemble two distinct products: a box containing a USB pen (product A) and a PCB board (product B), respectively. Steps required to obtain one finite piece of product A are:

1) take one empty box (box 1) and a cap (cap 1)
2) take one USB pen and the first layer of foam
3) assemble the box with the foam and the pen
4) take the second layer of foam and assemble it
5) fix the cap on the box

Steps required to obtain one finite piece of product B are:

1) take one pre-assembled box (box 2)
2) take one cap (cap 2)
3) fix the cap on the box

The robot's arms perform the picking of the box and the caps simultaneously. They then assemble it by making use of the assembly station indicated in Figure 4b. After the assembly of product A is completed, the newer piece is taken by the left arm of YuMi and put in a specific storage area near the right part of Figure 4b (the storage area is not visible in the same Figure). The items required to obtain product A and B are contained in specific buffers, located as indicated in Figure 4b. Some of the trajectories followed by both the human (his/her hands) and the robot (considering the end-effectors) during the assembly, are approximately depicted in Figure 4c. As can be seen, these trajectories cross a shared area. Notice that the locations of buffers are not selected in an ergonomic way, but the experimental set-up was designed mainly to show the validity of the developed approach.

Six volunteers were enrolled for the experiments and were divided into two groups I and II. For those in the group I, the approach presented in [11] was applied [1] for the computation of swept volumes adopting a basic linear kinematic model; while for those in group II, the hybrid approach described in Section IV-C was considered (with $P = 4$). Section V-A will compare performances obtained by the two groups, while Section V-B presents the results of some off-line simulations, comparing the performance achieved by all methods presented in Section IV, on the data (position in time of the operators) acquired on-line during the real experiments.

[1]Only the for the way swept volumes are generated, but not the way the robot's motion is controlled, since the approach of [10] is adopted as exposed at the beginning of this Section.

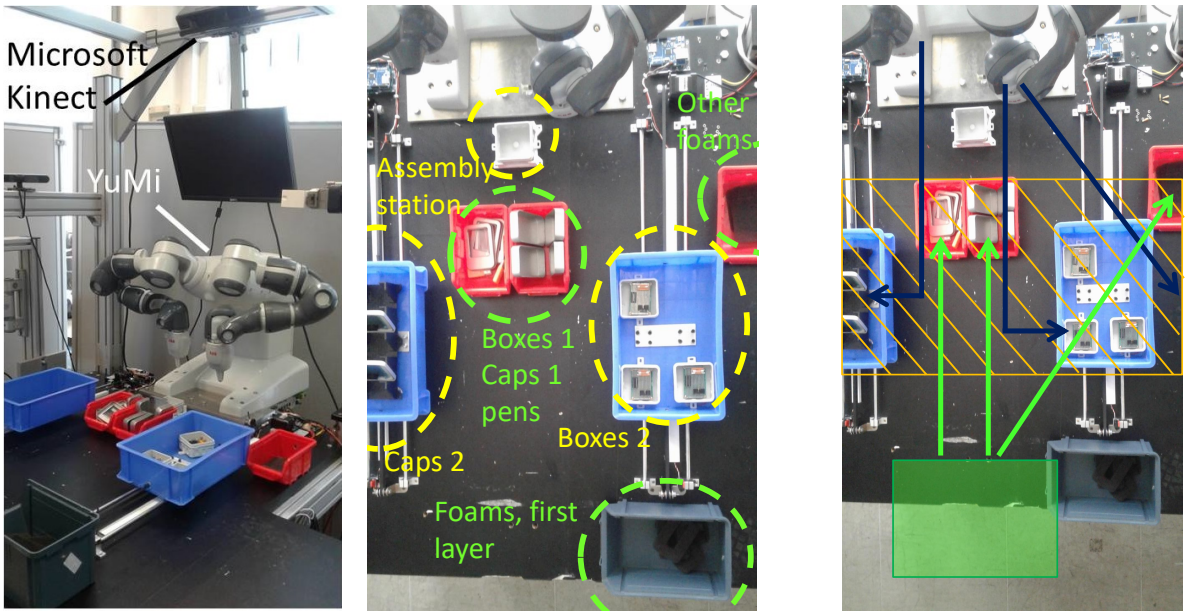

(a) YuMi of ABB, is visible in the centre; with a Microsoft Kinect vision system on top.

(b) Locations of buffers containing the items required to assemble product A and B.

(c) Some approximative trajectories followed by both the human (in clear green) and the robot (dark blue). The dashed orange area is the portion of space shared by the human and the robot, while the green shaded one is the portion of the space occupied by the operator's torso during the experiments.

Fig. 4: Experimental set-up considered for the experiments.

A. Real experiments

The sample time of the depth camera was set to 50 ms. When applying the hybrid method of Section IV, a newer Gaussian Process model for the three groups of joints is trained every 500 ms. Therefore, for every new training of the models, 10 newer samples are available. The training set has a fixed size equal to 100 samples. Newer samples replace 10 older ones every time an update of the model is invoked. Samples to replace are selected randomly with a uniform distribution in order to have a novel set with samples of both the recent and the remote past [2]. Each of the volunteers in the groups I and II was required to accomplish 5 assemblies, while the robot simultaneously accomplished the assembly of product B. The mean cycle time of the robot for the experiments of group II was about $8.59 \pm 1.3\%$ lower than the one related to experiments for group I, showing the beneficial effects of having a less conservative prediction of human motion. The mean time required to train a new model was 309.86 ms, with a standard deviation equal to 153.07 ms, which is compatible with the frequency selected for updating h_{GP}.

[2]In principle, it could be possible to consider the trace of $\underline{\underline{V}}_{k|K}$ and sample position to replace accordingly, i.e. trying to remove samples with an higher uncertainty. However, after a transient phase, Kalman Filter reaches a steady state for which the trace of the estimation covariance stops to changing significantly. Therefore, that approach would end up to be equivalent to sampling with a uniform distribution.

B. Off-line simulations

For every sample of the data logged on-line during the experiments, it is possible to compute $\epsilon^+ = \underline{\Delta}^+_{pred} - \underline{\Delta}^+_{real}$ and $\epsilon^- = \underline{\Delta}^-_{pred} - \underline{\Delta}^-_{real}$. $\underline{\Delta}^{+,-}_{pred}$ are the excursions predicted for every human articulation using h_{GP}, with the different methods described in Section IV; while $\Delta^{+,-}_{real}$ is the real excursion followed. The excursions $\Delta^{+,-}_{real}$ are computed according to the estimates $q_{1|1}, \cdots, q_{N|N}$ retrieved on-line by the Kalman filter during the experiments and saved for this off-line processing phase. Notice that it is a sufficient and necessary condition to require both $\epsilon^+ \geqslant 0$ and $\epsilon^- \geqslant 0$ for guaranteeing that the predicted excursion entirely contains the real followed trajectory. Moreover, the more ϵ^+ is positive and large, the more conservative the prediction was (the same applies for ϵ^-). Figures 2 and 3, report some statistics about ϵ^+ and ϵ^-, on the data of the experiments. As can be seen, the approach in [11] produces predictive excursions that almost always contain the real excursions of joints, even though the approach turns out to be very conservative, since $\epsilon^{+,-}$ are positive and assume big values. On the opposite, the methods proposed in Section IV result to produce lower $\epsilon^{+,-}$ which can be also negative sometimes. In particular, the hybrid approach of Section IV-C seems to be the one producing predictions with the best compromise between conservativeness and risk of violation. Surprisingly, in both in Figure 2 and 3 no significant differences can be detected when considering a specific method with different values for the order P. For the hybrid approach of Section IV-C, Figure 6 reports also the distance of the real positions of

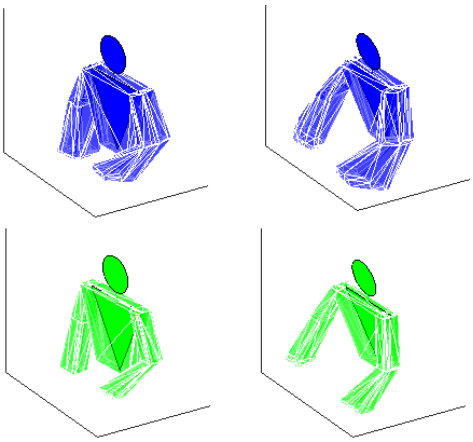

Fig. 5: Comparisons between the swept volumes obtained considering [11] (the blue ones on the first row) against those obtained applying the hybrid approach of Section IV $P = 4$ (the green ones on the second row), for two sampled instants of the logged data.

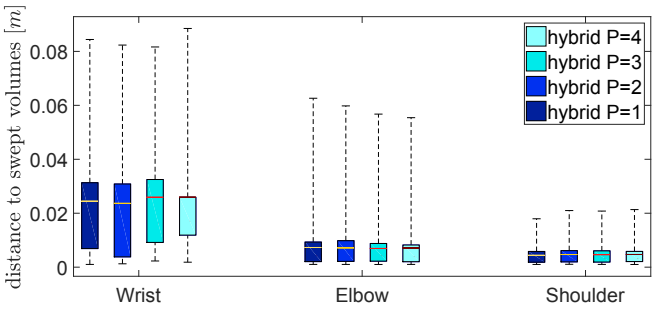

Fig. 6: Statistics about the distances between skeletal points and predicted swept volumes, in case of violation of the predicted joint excursion.

wrists, elbows and shoulders to the predicted swept volumes, considering only those samples for which $\epsilon^+ \leqslant 0$ or $\epsilon^- \leqslant 0$. As can be seen from the analysis of Figure 6, the violation of the predicted swept volumes by the real trajectory followed by skeletal points is in the order of few centimeters. Figure 5 reports also a visual comparison of some swept volumes computed with [11], w. r. t. the ones computed by the hybrid approach with a $P = 4$.

VI. Conclusions

This work presented a novel approach to human swept volumes computation, adopting a machine learning method. The experiments proved their validity in terms of reduced conservativeness, which reflects in an improved robotic motion control when sharing a common space with the human. In particular, the robot is allowed to undertake less severe corrective maneuvers about its cruise speed, completing faster the tasks assigned. As a matter for future studies, it could be interesting to study more in depth the correlation between the order of the Kalman filter adopted to retrieve newer samples and the order P of the Gaussian Process adopted, investigating if it is more efficient to increase the one or the other. Moreover, it could be interesting to use the learnt GP for propagating the a-posteriori estimates to obtain the a-priori one, i.e. those that the Kalman filter will correct according to the measures. This would avoid to adopt a generic kinematic model for the human, improving the tracking performance.

References

[1] S. Haddadin, M. Suppa, S. Fuchs, T. Bodenmüller, A. Albu-Schäffer, and G. Hirzinger, "Towards the robotic co-worker," in *Robotics Research*. Springer, 2011, pp. 261–282.

[2] D. Kulić and E. Croft, "Pre-collision safety strategies for human-robot interaction," *Autonomous Robots*, vol. 22, no. 2, pp. 149–164, 2007.

[3] R. Schiavi, A. Bicchi, and F. Flacco, "Integration of active and passive compliance control for safe human-robot coexistence," in *Robotics and Automation, 2009. ICRA'09. IEEE International Conference on*. IEEE, 2009, pp. 259–264.

[4] R. Mosberger and H. Andreasson, "An inexpensive monocular vision system for tracking humans in industrial environments." in *ICRA*, 2013, pp. 5850–5857.

[5] N. Najmaei, M. R. Kermani, and M. A. Al-Lawati, "A new sensory system for modeling and tracking humans within industrial work cells," *IEEE Transactions on Instrumentation and Measurement*, vol. 60, no. 4, pp. 1227–1236, 2011.

[6] M. Munaro, C. Lewis, D. Chambers, P. Hvass, and E. Menegatti, "Rgb-d human detection and tracking for industrial environments," in *Intelligent Autonomous Systems 13*. Springer, 2016, pp. 1655–1668.

[7] R. Urtasun, D. J. Fleet, and P. Fua, "3d people tracking with gaussian process dynamical models," in *Computer Vision and Pattern Recognition, 2006 IEEE Computer Society Conference on*, vol. 1. IEEE, 2006, pp. 238–245.

[8] Z. Wang, J. Kinugawa, H. Wang, and K. Kazahiro, "A human motion estimation method based on gp-ukf," in *Information and Automation (ICIA), 2014 IEEE International Conference on*. IEEE, 2014, pp. 1228–1232.

[9] X. Liu and J. Zhang, "Active learning for human action recognition with gaussian processes," in *Image Processing (ICIP), 2011 18th IEEE International Conference on*. IEEE, 2011, pp. 3253–3256.

[10] A. M. Zanchettin and P. Rocco, "Path-consistent safety in mixed human-robot collaborative manufacturing environments," in *2013 IEEE/RSJ Int. Conf. on Intelligent Robots and Systems*, Nov 2013, pp. 1131–1136.

[11] M. Ragaglia, A. M. Zanchettin, and P. Rocco, "Trajectory generation algorithm for safe human-robot collaboration based on multiple depth sensor measurements," *Mechatronics*, 2018.

[12] H. Täubig, B. Bäuml, and U. Frese, "Real-time swept volume and distance computation for self collision detection," in *Intelligent Robots and Systems (IROS), 2011 IEEE/RSJ International Conference on*. IEEE, 2011, pp. 1585–1592.

[13] C. E. Rasmussen, "Gaussian processes in machine learning," in *Advanced lectures on machine learning*. Springer, 2004, pp. 63–71.

[14] D. Duvenaud, "Automatic model construction with gaussian processes," Ph.D. dissertation, University of Cambridge, 2014.

[15] K. P. Murphy and S. Russell, "Dynamic bayesian networks: representation, inference and learning," 2002.